

Dear Author,

Here are the proofs of your article.

- You can submit your corrections **online**, via **e-mail** or by **fax**.
- For **online** submission please insert your corrections in the online correction form. Always indicate the line number to which the correction refers.
- You can also insert your corrections in the proof PDF and **email** the annotated PDF.
- For fax submission, please ensure that your corrections are clearly legible. Use a fine black pen and write the correction in the margin, not too close to the edge of the page.
- Remember to note the **journal title**, **article number**, and **your name** when sending your response via e-mail or fax.
- **Check** the metadata sheet to make sure that the header information, especially author names and the corresponding affiliations are correctly shown.
- **Check** the questions that may have arisen during copy editing and insert your answers/corrections.
- **Check** that the text is complete and that all figures, tables and their legends are included. Also check the accuracy of special characters, equations, and electronic supplementary material if applicable. If necessary refer to the *Edited manuscript*.
- The publication of inaccurate data such as dosages and units can have serious consequences. Please take particular care that all such details are correct.
- Please **do not** make changes that involve only matters of style. We have generally introduced forms that follow the journal's style. Substantial changes in content, e.g., new results, corrected values, title and authorship are not allowed without the approval of the responsible editor. In such a case, please contact the Editorial Office and return his/her consent together with the proof.
- If we do not receive your corrections **within 48 hours**, we will send you a reminder.
- Your article will be published **Online First** approximately one week after receipt of your corrected proofs. This is the **official first publication** citable with the DOI. **Further changes are, therefore, not possible.**
- The **printed version** will follow in a forthcoming issue.

Please note

After online publication, subscribers (personal/institutional) to this journal will have access to the complete article via the DOI using the URL: [http://dx.doi.org/\[DOI\]](http://dx.doi.org/[DOI]).

If you would like to know when your article has been published online, take advantage of our free alert service. For registration and further information go to: <http://www.springerlink.com>.

Due to the electronic nature of the procedure, the manuscript and the original figures will only be returned to you on special request. When you return your corrections, please inform us if you would like to have these documents returned.

Metadata of the article that will be visualized in OnlineFirst

ArticleTitle	Towards a better understanding of the Oulmes hydrogeological system (Mid-Atlas, Morocco)	
Article Sub-Title		
Article CopyRight	Springer-Verlag (This will be the copyright line in the final PDF)	
Journal Name	Environmental Earth Sciences	
Corresponding Author	Family Name	Wildemeersch
	Particle	
	Given Name	Samuel
	Suffix	
	Division	Hydrogeology and Environmental Geology, GEO3, ArGenCo
	Organization	University of Liege
	Address	Building B52/3 Sart-Tilman, Liege, 4000, Belgium
	Email	swildemeersch@ulg.ac.be
Author	Family Name	Orban
	Particle	
	Given Name	Philippe
	Suffix	
	Division	Hydrogeology and Environmental Geology, GEO3, ArGenCo
	Organization	University of Liege
	Address	Building B52/3 Sart-Tilman, Liege, 4000, Belgium
	Division	Aquapôle
	Organization	University of Liege
	Address	Liege, Belgium
Author	Family Name	Ruthy
	Particle	
	Given Name	Ingrid
	Suffix	
	Division	Hydrogeology and Environmental Geology, GEO3, ArGenCo
	Organization	University of Liege
	Address	Building B52/3 Sart-Tilman, Liege, 4000, Belgium
	Email	
Author	Family Name	Grière
	Particle	
	Given Name	Olivier
	Suffix	
	Division	
	Organization	G2H Conseils
	Address	29 Rue Blanche Hottinguer, Guermantes, 77600, France
	Email	
Author	Family Name	Olive
	Particle	

	Given Name	Philippe
	Suffix	
	Division	
	Organization	
	Address	1C Avenue du Léman, Thonon-Les-Bains, 74200, France
	Email	
Author	Family Name	El Youbi
	Particle	
	Given Name	Abdelkhalek
	Suffix	
	Division	
	Organization	Parc Industriel de Bouskoura, Eaux Minérales d'Oulmès
	Address	Casablanca, Morocco
	Email	
Author	Family Name	Dassargues
	Particle	
	Given Name	Alain
	Suffix	
	Division	Hydrogeology and Environmental Geology, GEO3, ArGEnCo
	Organization	University of Liege
	Address	Building B52/3 Sart-Tilman, Liege, 4000, Belgium
	Email	
Schedule	Received	13 December 2008
	Revised	
	Accepted	25 September 2009
Abstract	<p>Located in the Mid-Atlas (Morocco), the Oulmes plateau is famous for its mineral water springs “Sidi Ali” and “Lalla Haya” commercialised by the company “Les Eaux minérales d’Oulmès S.A”. Additionally, groundwater of the Oulmes plateau is intensively exploited for irrigation. The objective of this study, essentially performed from data collected during isotopic (summer 2004) and piezometric and hydrogeochemical field campaigns (spring 2007), is to improve the understanding of the Oulmes hydrogeological system. Analyses and interpretation of these data lead to the statement that this system is constituted by a main deep aquifer of large extension and by minor aquifers in a perched position. However, these aquifers interact enough to be in total equilibrium during the cold and wet period. As highlighted by isotopes, the origin of groundwater is mainly infiltration water except a small part of old groundwater with dissolved gas rising up from the granite through the schists.</p>	
Keywords (separated by '-')	Hydrogeological characterisation - Hydrogeochemistry - Isotopes - Morocco	
Footnote Information		

Journal: 12665
Article: 312



Author Query Form

**Please ensure you fill out your response to the queries raised below
and return this form along with your corrections**

Dear Author

During the process of typesetting your article, the following queries have arisen. Please check your typeset proof carefully against the queries listed below and mark the necessary changes either directly on the proof/online grid or in the 'Author's response' area provided below

Query	Details required	Author's response
1.	Please check and confirm the author names and initials are correct. Also please check and confirm the affiliation details are identified correctly.	
2.	Please check all the references are correctly identified.	
3.	References Winckel 2002 is cited in text but not provided in the reference list. Please provide reference in the list or delete these citations.	
4	Please check the equations are correct. It has symbol(ε) mismatch instead of δ .	

Towards a better understanding of the Oulmes hydrogeological system (Mid-Atlas, Morocco)

Samuel Wildemeersch · Philippe Orban ·
Ingrid Ruthy · Olivier Grière · Philippe Olive ·
Abdelkhalek El Youbi · Alain Dassargues

Received: 13 December 2008 / Accepted: 25 September 2009
© Springer-Verlag 2009

Abstract Located in the Mid-Atlas (Morocco), the Oulmes plateau is famous for its mineral water springs “Sidi Ali” and “Lalla Haya” commercialised by the company “Les Eaux minérales d’Oulmès S.A”. Additionally, groundwater of the Oulmes plateau is intensively exploited for irrigation. The objective of this study, essentially performed from data collected during isotopic (summer 2004) and piezometric and hydrogeochemical field campaigns (spring 2007), is to improve the understanding of the Oulmes hydrogeological system. Analyses and interpretation of these data lead to the statement that this system is constituted by a main deep aquifer of large extension and by minor aquifers in a perched position. However, these aquifers interact enough to be in total equilibrium during the cold and wet period. As highlighted by isotopes, the origin of groundwater is mainly infiltration water except a small part of old groundwater with dissolved gas rising up from the granite through the schists.

Keywords Hydrogeological characterisation · Hydrogeochemistry · Isotopes · Morocco

Introduction

All over the world, water resources are under serious pressure and their efficient management and protection constitute a key issue for the future. This is especially the case in country with semi-arid zones where such resources are strongly exploited for irrigation. The first step in order to manage and protect groundwater resources consists in understanding precisely the local hydrogeological system. It can be particularly uneasy to reach this objective in fractured hard rock geological formations.

The Oulmes plateau, located in the Mid-Atlas (Morocco), with its famous “Sidi Ali” and “Lalla Haya” mineral water springs, is a particularly challenging case study. The main objective of this work is to improve the understanding of the hydrodynamic and hydrogeochemical processes occurring in a very complex geological and hydrogeological system located in a contrasting climate zone with increasing man-induced pressures. These pressures, including groundwater extraction for commercialisation and irrigation as well as use of fertilizers for farming, are suspected of modifying the hydrogeological system in terms of quantity and quality, which justifies the necessity of such a scientific study.

Previous private and unpublished hydrogeological studies, including local piezometric surveys and hydrogeochemical studies, lead to a conceptual and general statement that the groundwater pumped in wells owned by the company comes from a mixing of shallow groundwater (with the resulting possible contamination), intermediate groundwater fairly mineralised and deep mineralised

S. Wildemeersch (✉) · P. Orban · I. Ruthy · A. Dassargues
Hydrogeology and Environmental Geology, GEO3, ArGenCo,
University of Liege, Building B52/3 Sart-Tilman,
4000 Liege, Belgium
e-mail: swildemeersch@ulg.ac.be

O. Grière
G2H Conseils, 29 Rue Blanche Hottinguer,
77600 Guermantes, France

P. Olive
1C Avenue du Léman, 74200 Thonon-Les-Bains, France

A. El Youbi
Parc Industriel de Bouskoura, Eaux Minérales d’Oulmès,
Casablanca, Morocco

P. Orban
Aquapôle, University of Liege, Liege, Belgium

groundwater with dissolved gas in variable proportions linked to the granitic intrusion. However, these previous studies lacked data and could not be considered as exhaustive enough to produce results with a high degree of certainty. The present study, focused mainly on the “Sidi Ali” spring, is based on a larger set of data collected during field campaigns carried out during summer 2004 and spring 2007. Among others, these campaigns produced measured groundwater levels and groundwater samples from many springs and wells. Temperature and precipitations data ranging from October 1985 and September 2006 were also collected in the “Bâa” farm located at immediate proximity of the “Sidi Ali” spring. Thanks to this large set of data, a comprehensive hydrogeological study including hydrodynamic, hydrogeochemical, and isotopic parts was undertaken providing the results described here below.

Study zone

The Oulmes plateau (Mid-Atlas, Morocco), located 150 km southeast of Rabat, is entirely included in the

Moroccan central plateau (Termier 1936; Beaudet 1969; Michard 1976). The plateau is limited by the Afcâl wadi to the north, the Boulahmayal wadi to the south and to the west, and a main road in the east (Agard et al. 1950) (Fig. 1). The altitudes of the Oulmes plateau range from 450 m (in the valley of the Boulahmayal wadi) to 1,250 m (near the city of Oulmes) while the most frequent altitude is 1,080 m (Dadi 1998).

The contrasting climate is characterised by a warm and dry season from May to September, and a cold and wet season from October to April. The mean annual temperature and precipitations, calculated for the 1985–2006 period, are respectively 16.9°C and 635 mm. About 90% of precipitations are recorded during the cold and wet period. Except the Afcâl and the Boulahmayal wadis, all others wadis are not perennial and they flow only during the wet season.

Water resources of the Oulmes plateau are intensively exploited. Mineral waters from the “Sidi Ali” and “Lalla Haya” springs are both commercialised by the company “Les Eaux Minérales d’Oulmès S.A”, respectively, under the names of “Sidi Ali” and

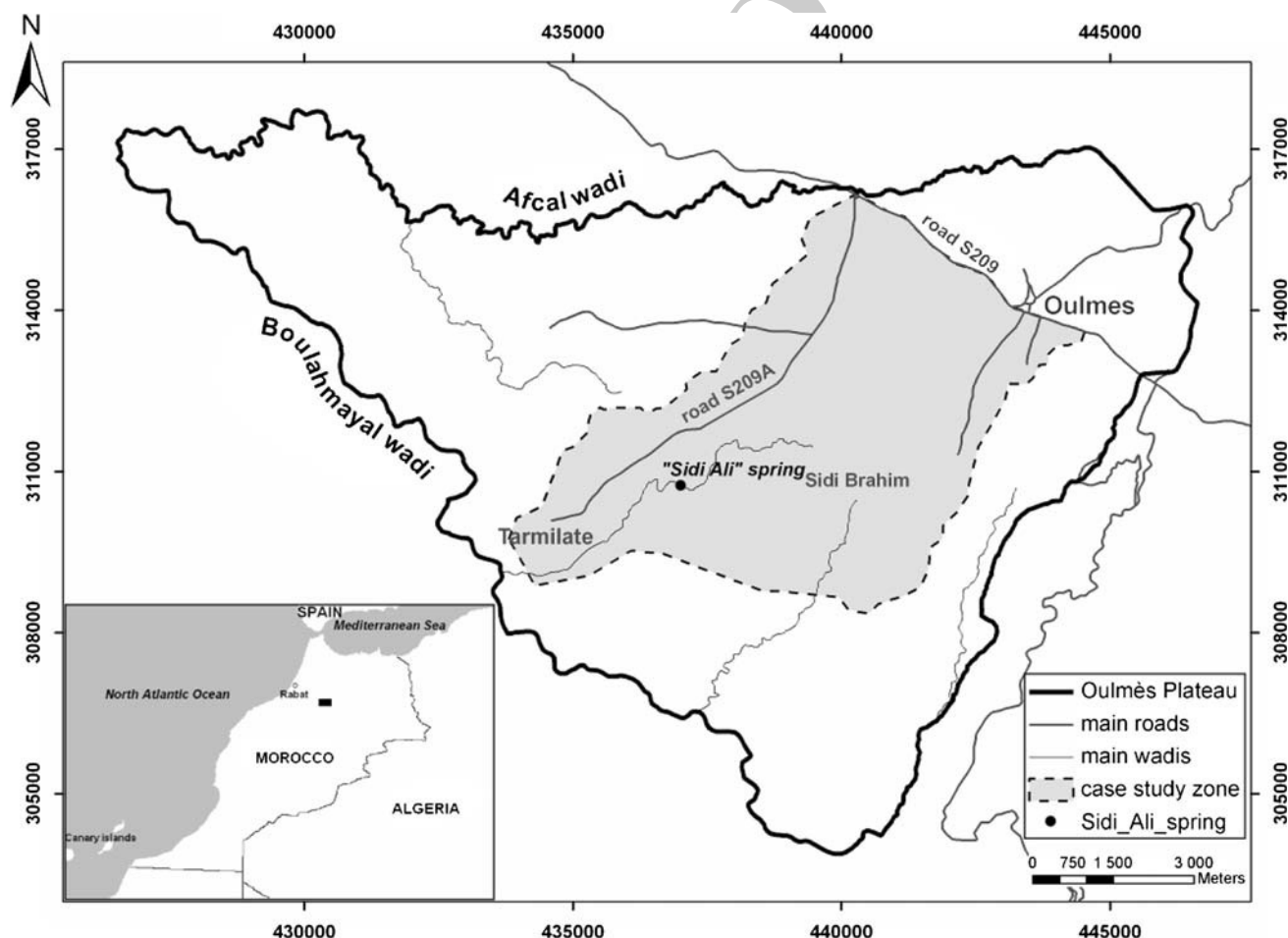


Fig. 1 Location of the Oulmes plateau and the study zone

“Oulmès” but groundwater is also exploited for intensive irrigation to cultivate various fruits species in modern orchards producing early fruits for Europe. Additionally, private and public wells of the “Office National de l’Eau Potable” (ONEP) located all over the zone but mainly near the town of Oulmes produce water supply for local inhabitants.

Geological and hydrogeological settings

Geological setting

Geologically, the Oulmes plateau is located at the northeast of the Khouribga-Oulmes anticlinorium and it includes two main types of geological formations: a central plutonic

granite formation (Fig. 2, A) surrounded by schists formations (Fig. 2, B). Eastwards from these schists formations, quartzitic formations (Fig. 2, C) are outcropping together with shales with limestone and sandstone nodules (Fig. 2, D) and limestones (Fig. 2, E).

The Oulmes granite outcrops on about 30 km² with an elliptic form oriented NNE–SSW with a large axis of 8.5 km and a small axis of 4.25 km (Diot et al. 1987). This plutonic intrusion occurred 298 My ago (Gmira 1996) along a subvertical sinistral shear zone oriented N10E and generated during the Hercynian tectonic phase (Diot et al. 1987; Gmira 1996). This phase, characterised by a regional compression oriented NW–SE (Lagarde 1985; Diot et al. 1987), folded and faulted the zone which had previously been folded by the Ante-Visean tectonic phase (Lagarde 1985; Tahiri 1991).

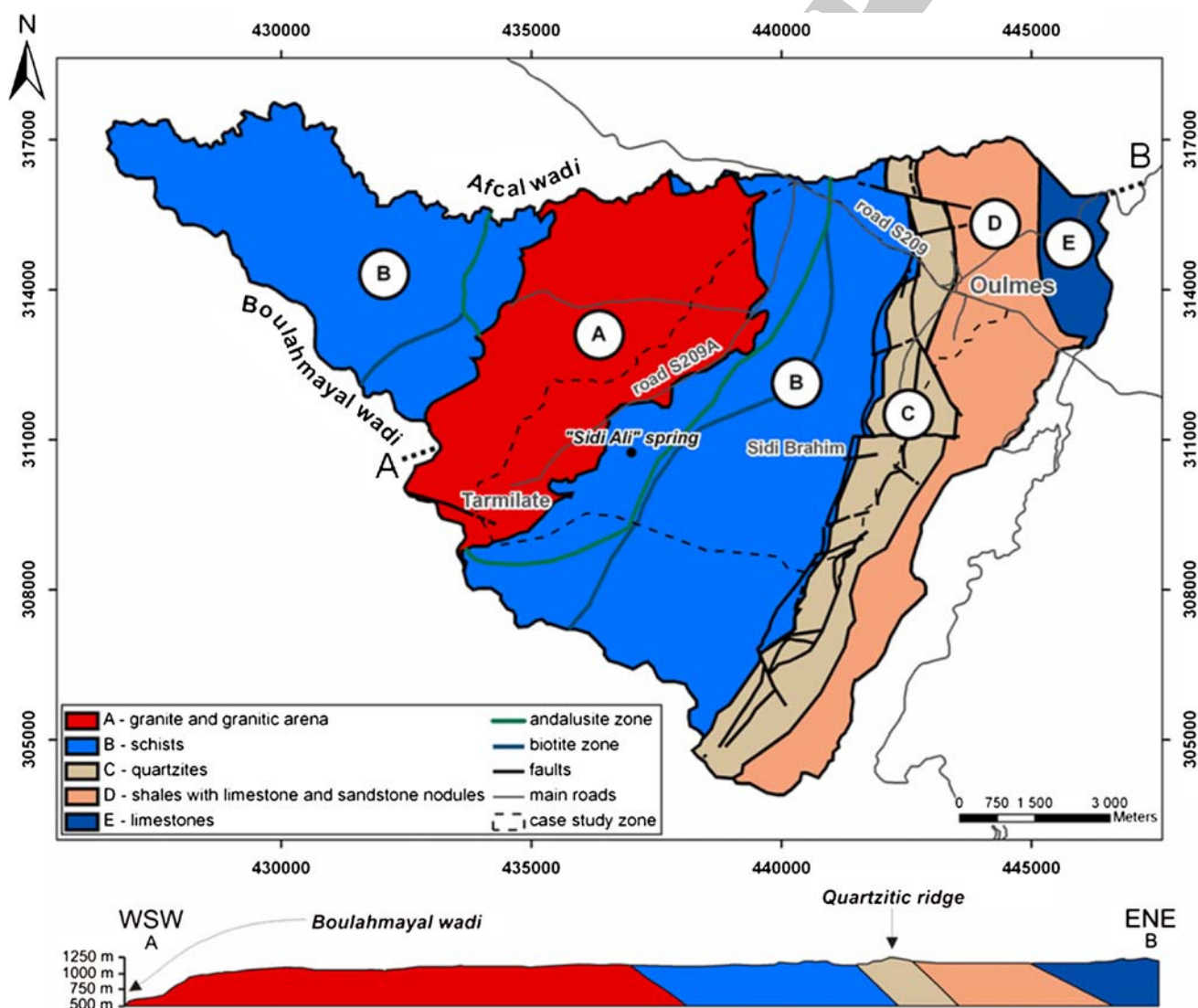


Fig. 2 Geological schema and cross-section of the Oulmes plateau showing mainly the Oulmes granite and the Palaeozoic formations [modified from (Baudin et al. 2001)]

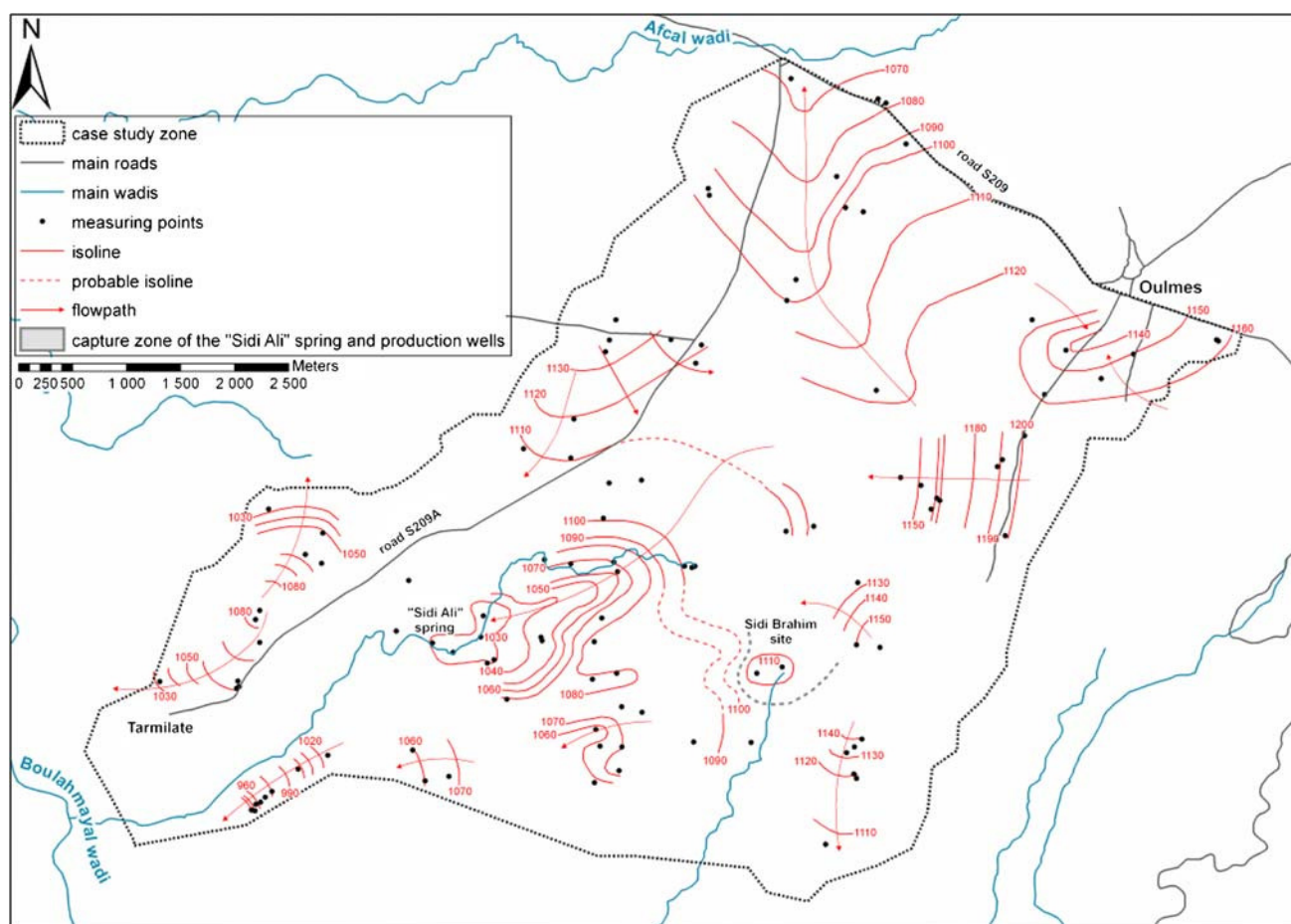


Fig. 3 Piezometric map of the study zone in March 2007 (isoline interval = 10 m)

The Palaeozoic schists formations, predominantly Ordovician, are the results of the metamorphism induced in the formations surrounding the granitic intrusion. This metamorphism, locally hydrothermal, increases as the rocks are close to the granitic intrusion (Michard 1976; Boutaleb 1988; Gmira 1996). The most metamorphosed zones are the andalusite zone and the biotite zone. Beyond these zones, less metamorphosed zones are found which are the green mica zone and the chlorite zone (Boutaleb 1988; Baudin et al. 2001).

Eastwards, the quartzitic formations form a main topographical ridge of the plateau. Towards the east and beyond these erosion resistant formations, Silurian and Devonian shales with limestone and sandstone nodules are found. In the extreme northeast of the zone, Visean limestones are observed in unconformity with the former formations because of the Ante-Visean tectonic phase. Consequently, the Tournaisian formations are missing on the Oulmes plateau. Volcanic and superficial formations such as the pinkish granitic gravely sands arena, resulting from the granite alteration and lying on a wide outcropping surface with a mean thickness of 0.6 m (Agard et al. 1950), are also present in the zone.

Hydrogeological setting

The main hydrogeological units of the Oulmes plateau can be considered as: (1) the superficial formations, characterised by a granular porosity, and (2) the fissured granitic and schists formations, essentially characterised by a fracture porosity.

The superficial formations, resulting from the granite, schists and quartzites weathering constitute very thin shallow aquifers. The granitic and schists formations are considered as aquifers only when a significant hydraulic conductivity is induced by interconnected fissure networks. The main measured fracture directions of the case study zone are orientated N10–N30 and N120–N140 and they are mostly subvertical (Dadi 1998). Pumping tests performed in the case study zone provide an average hydraulic conductivity of 10^{-5} m/s.

The “Sidi Ali” spring is currently exploited and bottled by the company “Les Eaux Minérales d’Oulmès S.A” thanks to wells drilled in metamorphosed schists very close to the Oulmes granite (andalusite zone). Consequently, the original “Sidi Ali” spring does not flow anymore, proving that pumpings have already modified the original

Table 1 Mean annual actual evapotranspiration (AEvT) and mean annual available water (W_a) calculated using the Thornthwaite method for three different values of maximum soil moisture storage capacity (STO_{max})

STO_{max} (mm)	AEvT (mm)	W_a (mm)
100	366	269
175	429	205
250	457	158

hydrogeological system. The company owns also production wells on the “Sidi Brahim” site located to the east from the “Sidi Ali” site (Fig. 1).

Materials and methods

Three kinds of data were collected for this study: isotopic data, hydrogeochemical data and piezometric data. Groundwater samples used for isotopic analyses were collected during a field campaign carried out in summer 2004. These isotopic samples were taken from 15 wells and springs chosen at different altitudes and located over the whole Mid-Atlas. The isotopic samples, representative of small watersheds and representative of precipitations, were analysed following standard procedures in Hydroisotop GmbH laboratory in Schweitenkirchen (Germany).

Water levels measurements and sampling of groundwater for geochemical analyses were performed during a field campaign in spring 2007. These 110 geochemical samples were taken manually from springs, shallow and deep wells without any pumping (except for three wells of the company). The piezometric head were measured with a piezometric probe and the hydrogeochemical analyses of major ions were performed using standard techniques in the laboratory of the University of Liege. The acceptable error on the ion balance of each sample is taken at 5%.



Fig. 4 Observed flow in a wadi during a heavy precipitations event

Results

Piezometric map

The piezometric map of the study zone (Fig. 3) was plotted including both static heads measured in private wells and dynamic heads measured in the three production wells of the company producing at this period (March 2007).

The piezometric map indicates that the topography strongly influences the piezometric heads which are underlined by steeper hydraulic gradients near crests. Groundwater, as surface waters, is drained by two main wadis which are the Afcad northward and the Boulahmayal southward and westward. Consequently, groundwater flow occurs to the north and to the southwest to join, respectively, the Afcad and the Boulahmayal wadis. Where groundwater is not directly drained by these wadis, it is drained by their main tributaries. Groundwater flow occurs also from east to west along the principal ridge of the Oulmes plateau which constitutes both a hydrological and a hydrogeological limit. Influence of the pumping is clearly visible through the cones of depression induced in Sidi Ali and Sidi Brahim sites. Furthermore, the Sidi Brahim pumping influences the hydrogeological system of the “Sidi Ali” spring by capturing a part of the groundwater that would flow naturally towards the “Sidi Ali” spring. The “Sidi Ali” groundwater capture zone as delineated from this piezometric map covers 10.94 km².

Annual groundwater budget

An annual groundwater budget is established for the “Sidi Ali” spring capture zone in order to estimate the infiltration

Table 2 Required infiltration surface ($S_{required}$) calculated for the three values of maximum soil moisture storage capacity (STO_{max}) and the three distributions of the available water (W_a) into runoff (R) and infiltration (I)

	R (mm)	I (mm)	$S_{required}$ (km ²)
$STO_{max} = 100 \text{ mm} \rightarrow W_a = 269 \text{ mm}$			
$R = 2/3 \text{ of } W_a$	179	90	2.98
$R = 3/4 \text{ of } W_a$	202	67	4.00
$R = 7/8 \text{ of } W_a$	235	34	7.88
$STO_{max} = 175 \text{ mm} \rightarrow W_a = 205 \text{ mm}$			
$R = 2/3 \text{ of } W_a$	137	68	3.94
$R = 3/4 \text{ of } W_a$	154	51	5.25
$R = 7/8 \text{ of } W_a$	179	26	10.31
$STO_{max} = 250 \text{ mm} \rightarrow W_a = 158 \text{ mm}$			
$R = 2/3 \text{ of } W_a$	105	53	5.06
$R = 3/4 \text{ of } W_a$	119	39	6.87
$R = 7/8 \text{ of } W_a$	138	20	13.40

Table 3 Temperature (T in $^{\circ}\text{C}$), electrical conductivity (EC in $\mu\text{S}/\text{cm}$), pH and concentrations in main chemical species (in mg/l) of each groundwater sample collected during the field campaign

Well ID	Lithological unit	$T(^{\circ}\text{C})$	EC ($\mu\text{S}/\text{cm}$)	pH ^a	Ca^{2+} (mg/l)	Mg^{2+} (mg/l)	Na^{+} (mg/l)	K^{+} (mg/l)	Fe (mg/l)	Cl^{-} (mg/l)	SO_4^{2-} (mg/l)	NO_2^{-} (mg/l)	NO_3^{-} (mg/l)	CO_3^{2-} (mg/l)	HCO_3^{-} (mg/l)	CO_2 (mg/l)
PB1	3	19.2	386.00	8.28	27.09	10.48	35.73	2.32	0.49	22.86	65.18	≤ 0.200	3.01	1.04	98.95	0.40
PB2	3	18.0	334.00	8.40	24.25	10.07	30.78	1.35	1.31	13.89	51.98	≤ 0.200	≤ 0.300	1.51	108.95	0.30
PB3	3	17.7	319.30	7.91	27.77	9.32	22.20	2.47	2.10	12.48	33.07	≤ 0.200	15.22	0.51	113.52	1.00
PB5	3	17.9	374.00	8.36	26.29	9.28	37.58	1.64	1.59	21.56	58.56	≤ 0.200	≤ 0.300	1.38	109.25	0.30
PB6	3	17.5	443.00	8.11	32.03	11.49	42.30	1.58	0.26	21.95	91.83	≤ 0.200	1.46	0.73	103.28	0.60
PB8	3	18.1	376.00	7.99	24.47	10.48	33.53	2.52	17.30	19.05	89.43	≤ 0.200	1.51	0.37	68.71	0.50
PB11	3	16.8	444.00	8.26	46.08	15.68	22.59	1.96	1.38	15.74	78.32	≤ 0.200	0.92	1.45	144.49	0.60
PB12	3	15.4	316.00	8.20	18.98	9.93	30.26	2.33	1.83	14.60	52.78	≤ 0.200	≤ 0.300	0.82	93.34	0.40
PB17	3	13.9	219.90	8.07	16.83	5.80	18.43	2.62	16.40	7.40	22.71	≤ 0.200	≤ 0.300	0.59	90.17	0.50
PB20	3	15.9	173.80	7.66	10.05	4.42	18.05	0.86	1.44	12.29	18.48	≤ 0.200	8.08	0.11	44.87	0.70
PB24	3	17.6	403.00	8.15	39.34	12.90	25.04	1.35	0.38	13.07	88.62	≤ 0.200	≤ 0.300	0.82	105.53	0.50
PB25	3	17.1	417.50	8.32	43.98	11.51	25.48	1.85	0.58	12.21	74.87	≤ 0.200	0.72	1.57	135.71	0.50
PB26	3	16.6	371.00	7.99	30.46	10.92	25.37	1.62	1.31	11.23	106.00	≤ 0.200	1.49	0.30	55.42	0.40
PB27	3	17.3	300.20	8.33	26.02	11.99	18.91	1.48	1.27	11.17	18.92	≤ 0.200	0.86	1.68	142.78	0.50
PB28	3	16.6	354.00	8.16	37.01	11.24	21.01	2.09	2.08	9.35	23.96	≤ 0.200	1.17	1.39	173.88	0.80
SA	2	17.8	239.30	7.76	16.68	7.06	21.81	1.38	4.11	12.31	37.38	≤ 0.200	≤ 0.300	0.26	82.37	1.00
P25	2	20.7	230.10	7.63	12.15	6.88	21.91	3.57	5.75	12.58	35.42	≤ 0.200	≤ 0.300	0.16	69.14	1.10
SI1	1	13.6	120.00	7.45	6.82	1.84	13.42	1.24	0.14	7.86	3.65	≤ 0.200	19.70	0.05	30.36	0.80
SI3	2	20.3	139.00	7.45	4.43	2.17	19.47	1.42	0.07	10.20	3.70	≤ 0.200	21.47	0.05	32.80	0.80
F4	2	19.0	302.20	7.44	14.78	9.97	26.50	2.89	19.10	13.99	87.84	≤ 0.200	1.24	0.05	31.58	0.80
F6	2	17.7	350.00	6.80	21.21	11.75	24.56	3.10	0.63	13.72	128.09	≤ 0.200	2.91	≤ 0.050	≤ 0.050	0.00
F7	2	18.2	267.70	7.82	13.73	7.41	26.41	3.42	1.86	24.11	41.85	≤ 0.200	0.83	0.22	60.48	0.60
F8	3	18.9	338.00	7.87	20.08	12.19	28.76	2.62	5.53	13.43	82.87	≤ 0.200	≤ 0.300	0.31	74.93	0.70
F9	2	19.0	269.30	7.92	12.38	8.56	28.25	2.86	6.59	14.33	47.06	≤ 0.200	≤ 0.300	0.36	77.24	0.60
X2	3	15.8	166.50	7.87	10.90	5.39	16.26	0.93	0.23	7.64	19.10	≤ 0.200	3.43	0.26	62.86	0.60
X4	1	12.7	127.00	7.33	7.30	1.71	13.52	1.33	14.50	8.68	4.16	≤ 0.200	21.76	0.04	30.42	1.00
X7	1	17.3	613.00	7.65	36.65	11.73	66.18	5.82	0.15	71.92	44.57	≤ 0.200	108.88	0.13	54.57	0.90
X10	3	14.8	174.30	6.38	11.64	6.85	7.55	1.12	0.18	10.43	18.60	≤ 0.200	48.68	≤ 0.050	≤ 0.050	0.00
X13	1	18.6	157.10	7.83	15.19	1.24	13.69	2.00	0.20	6.99	3.04	≤ 0.200	21.69	0.20	54.44	0.60
X3	1	14.0	165.50	7.61	9.12	2.38	19.02	1.05	0.26	13.39	2.88	≤ 0.200	25.79	0.09	37.62	0.60
X5	1	13.2	133.70	7.53	7.14	1.80	16.40	0.99	1.07	7.93	2.71	≤ 0.200	22.05	0.07	37.62	0.80
X9	3	13.5	187.10	4.50	5.67	8.02	10.51	2.65	0.77	15.16	51.07	≤ 0.200	1.83	≤ 0.050	≤ 0.050	0.00
X11	3	17.4	165.30	7.39	8.70	4.88	15.16	0.76	0.94	12.12	20.90	≤ 0.200	16.11	0.04	30.36	0.90
X12	3	18.2	402.00	7.76	47.59	11.32	22.15	4.63	1.45	11.66	24.90	≤ 0.200	5.51	0.64	199.85	2.40
X14	1	16.5	158.30	7.35	10.65	2.81	17.43	1.44	0.40	6.81	3.20	≤ 0.200	19.24	0.07	59.56	1.90

Table 3 continued

Well ID	Lithological unit	T(°C)	EC (μS/cm)	pH ^a	Ca ²⁺ (mg/l)	Mg ²⁺ (mg/l)	Na ⁺ (mg/l)	K ⁺ (mg/l)	Fe (mg/l)	Cl ⁻ (mg/l)	SO ₄ ²⁻ (mg/l)	NO ₂ ⁻ (mg/l)	NO ₃ ⁻ (mg/l)	CO ₃ ²⁻ (mg/l)	HCO ₃ ⁻ (mg/l)	CO ₂ (mg/l)
X15	1	16.2	144.60	7.36	16.82	1.35	9.93	2.36	0.42	6.43	4.89	≤0.200	3.40	0.09	68.10	2.10
X16	2	15.4	129.40	7.01	10.19	2.07	10.74	1.74	0.18	7.08	2.26	≤0.200	27.94	0.02	30.42	2.10
X17	2	18.5	399.00	7.88	39.42	9.26	30.72	6.16	0.22	27.42	8.64	≤0.200	12.31	0.72	171.62	1.60
X19	2	18.2	471.00	8.36	47.55	9.85	26.14	23.09	0.15	24.64	36.37	≤0.200	2.75	2.43	192.47	0.60
X21	1	15.5	268.10	7.51	20.34	5.03	20.33	3.76	0.10	18.17	11.16	≤0.200	66.85	0.06	31.58	0.70
X22	2	18.5	215.10	8.02	17.73	6.06	17.99	1.44	1.10	9.68	14.58	≤0.200	≤0.300	0.56	97.55	0.70
X23	3	17.7	227.60	8.06	30.95	5.15	6.59	1.04	2.41	7.49	30.09	≤0.200	≤0.300	0.54	85.41	0.50
X25	3	-	117.50	5.95	5.66	5.16	7.20	0.53	0.33	11.85	22.28	≤0.200	9.44	≤0.050	≤0.050	0.00
X26	4	-	168.80	7.44	11.81	7.35	6.62	1.71	0.25	13.28	1.85	≤0.200	36.38	0.05	30.36	0.80
X27	5	-	432.80	8.22	73.54	9.58	5.99	≤0.050	0.41	7.09	50.30	≤0.200	4.18	1.82	198.63	0.80
SB1	3	18.5	226.50	7.81	20.29	6.18	17.57	1.10	1.44	9.46	25.31	≤0.200	≤0.300	0.33	91.94	1.00
SB3	3	19.8	248.90	7.76	26.49	5.66	17.13	≤0.050	4.61	9.19	21.86	≤0.200	≤0.300	0.35	110.23	1.30
SB4	3	18.8	208.20	7.45	14.00	5.07	17.83	4.32	0.74	10.33	26.49	≤0.200	1.87	0.11	71.70	1.80
P1	2	17.5	148.90	6.95	6.62	2.37	18.31	1.42	0.61	8.19	2.91	≤0.200	29.54	0.02	36.52	2.90
P35-S3	1	12.8	256.20	7.58	23.73	4.97	19.61	1.57	0.05	25.57	12.99	2.02	19.04	0.14	64.32	1.20
P10	2	18.0	161.30	7.42	12.76	2.79	13.57	2.40	0.04	7.69	18.13	0.47	14.47	0.06	42.55	1.10
P11	2	15.9	148.70	7.54	18.69	2.01	7.07	2.29	0.03	5.68	1.85	≤0.200	24.63	0.10	53.41	1.10
P12	2	18.9	210.50	6.68	9.51	6.13	17.64	2.42	0.48	10.23	64.13	≤0.200	6.86	≤0.050	≤0.050	0.00
P13	2	16.5	213.80	7.50	10.76	5.74	20.45	4.55	0.46	15.17	29.02	≤0.200	10.62	0.09	51.03	1.10
P14	2	19.1	152.20	7.55	10.83	7.26	6.52	3.88	3.10	8.21	2.33	≤0.200	10.53	0.13	67.98	1.30
PB15	3	17.3	401.00	8.00	48.04	10.81	19.94	1.59	21.20	11.79	57.36	≤0.200	3.07	0.88	159.12	1.10
P17	2	17.3	238.30	7.57	15.66	7.81	19.77	0.96	0.24	19.18	15.11	≤0.200	13.38	0.16	80.11	1.50
P18	3	17.1	181.20	7.61	12.67	5.56	15.73	1.44	3.58	9.58	14.35	≤0.200	≤0.300	0.18	78.89	1.40
P19-S5	3	13.8	228.50	7.49	17.24	7.73	14.33	1.70	0.74	12.36	35.81	≤0.200	11.73	0.09	54.69	1.20
P20	2	18.0	202.90	7.72	15.85	5.96	18.26	1.33	1.30	10.32	14.45	≤0.200	≤0.300	0.27	93.28	1.20
P26b	4	16.1	250.90	7.95	38.83	6.68	6.80	0.99	1.76	8.98	2.02	≤0.200	3.86	0.69	139.98	1.10
P28	1	20.9	1173.00	7.56	88.13	21.24	103.23	4.86	0.17	156.19	33.40	≤0.200	279.39	0.10	49.75	1.00
P30	1	17.7	862.00	8.01	64.90	17.01	94.04	5.74	0.14	86.72	135.69	≤0.200	38.90	0.86	151.81	1.00
P31	1	18.8	1684.50	8.40	81.92	23.51	288.74	16.90	0.11	238.89	62.72	≤0.200	60.88	6.95	501.51	1.40
P32	1	17.7	773.30	8.21	80.84	6.57	75.94	10.28	0.21	57.49	78.07	≤0.200	61.45	1.99	222.65	1.00
P34	1	15.0	540.00	7.81	29.09	7.48	69.72	3.38	0.22	45.29	85.46	≤0.200	55.82	0.22	62.92	0.70
P36	1	15.3	227.30	7.29	15.09	5.24	17.10	3.86	0.31	24.90	6.12	1.16	80.90	≤0.050	≤0.050	0.00
P37	2	18.3	140.20	7.41	13.72	1.75	10.16	2.03	0.04	6.33	2.16	≤0.200	26.04	0.06	41.34	1.10
P40	3	16.5	244.50	8.00	27.50	5.40	16.13	1.17	0.94	8.00	19.63	≤0.200	2.94	0.62	112.06	0.80
P43	1	18.2	116.90	7.26	7.33	1.38	10.44	3.53	≤0.005	10.50	1.76	≤0.200	41.65	≤0.050	≤0.050	0.00
P45	3	19.0	188.90	7.63	22.45	5.49	5.67	2.37	8.41	8.92	18.08	≤0.200	6.36	0.16	66.70	1.10

Table 3 continued

Well ID	Lithological unit	T(°C)	EC (μS/cm)	pH ^a	Ca ²⁺ (mg/l)	Mg ²⁺ (mg/l)	Na ⁺ (mg/l)	K ⁺ (mg/l)	Fe (mg/l)	Cl ⁻ (mg/l)	SO ₄ ²⁻ (mg/l)	NO ₂ ⁻ (mg/l)	NO ₃ ⁻ (mg/l)	CO ₃ ²⁻ (mg/l)	HCO ₃ ⁻ (mg/l)	CO ₂ (mg/l)
P46	3	16.6	149.30	7.71	13.89	3.71	9.69	3.74	0.03	6.89	14.00	≤0.200	1.64	0.17	60.60	0.80
P47	3	15.0	125.60	5.84	6.29	5.02	6.89	1.06	0.53	9.82	20.50	≤0.200	20.12	≤0.050	≤0.050	0.00
P48	3	16.6	309.90	3.41	16.32	10.81	11.14	4.20	1.39	8.42	108.85	≤0.200	≤0.300	≤0.050	≤0.050	0.00
P49	3	16.2	146.20	5.00	9.10	3.69	9.17	2.00	0.79	11.75	37.08	≤0.200	6.21	≤0.050	≤0.050	0.00
X43	3	16.3	146.90	7.24	9.59	5.37	≤0.020	2.59	2.59	7.94	25.86	≤0.200	11.91	≤0.050	≤0.050	0.00
P64	1	16.3	230.90	10.00	28.86	2.22	12.83	3.00	0.85	9.45	9.83	≤0.200	45.88	14.90	27.01	0.00
P69	5	—	147.20	7.49	15.34	4.33	7.60	0.77	4.89	5.24	22.50	≤0.200	≤0.300	0.09	51.03	1.20
P74	4	—	150.60	7.66	13.12	6.78	7.05	0.85	1.83	5.55	22.32	≤0.200	≤0.300	0.14	53.35	0.80
P79	2	16.5	459.00	7.94	56.00	7.50	18.37	11.56	3.60	14.68	51.10	≤0.200	74.51	0.46	95.35	0.80
P100	3	18.3	259.50	8.12	22.55	9.80	19.75	1.32	7.79	10.29	18.44	≤0.200	0.79	0.94	128.52	0.70
P101	4	16.0	230.70	7.87	21.67	9.26	11.19	1.00	0.17	4.94	47.11	≤0.200	1.76	0.30	72.49	0.70
P105	4	16.4	151.80	7.67	14.96	4.80	8.72	0.77	1.65	6.41	20.25	≤0.200	6.14	0.13	50.91	0.80
P106	4	16.5	143.00	7.53	11.14	4.95	8.90	0.97	≤0.005	7.04	4.38	≤0.200	28.69	0.07	38.84	0.80
P107	5	—	390.00	8.12	55.44	13.18	7.64	2.81	3.39	10.30	30.81	≤0.200	6.46	1.37	188.57	1.00
P108	5	—	226.80	7.92	36.92	3.47	3.68	1.06	5.10	6.99	16.62	≤0.200	28.01	0.36	78.46	0.70
PB21	3	16.2	463.00	8.13	48.69	15.20	27.59	1.22	2.86	14.99	102.10	≤0.200	1.48	1.02	136.87	0.70
X29	3	—	249.20	8.09	25.28	5.80	19.75	1.90	9.68	10.39	20.02	≤0.200	≤0.300	0.82	120.23	0.70
X30	3	—	210.50	8.03	18.59	4.26	16.35	3.39	0.07	10.24	21.67	≤0.200	5.47	0.48	80.66	0.50
X31	3	—	303.80	7.75	29.02	12.76	8.06	5.99	9.21	6.90	74.42	≤0.200	5.62	0.24	77.49	1.00
X33	2	—	249.70	7.65	11.51	8.46	25.43	2.47	4.02	23.26	18.03	≤0.200	≤0.300	0.23	92.18	1.40
X34	2	—	371.00	8.06	36.26	7.62	29.30	4.41	0.26	20.73	25.16	≤0.200	7.22	1.02	161.26	1.00
X35	2	—	295.90	7.85	12.90	10.28	29.72	2.25	1.68	36.12	16.14	≤0.200	2.76	0.37	94.31	0.90
X36	2	—	267.20	7.76	11.23	9.07	28.86	1.34	0.23	30.38	11.51	≤0.200	11.38	0.27	85.96	1.00
X37	2	—	290.70	7.81	12.02	9.30	32.45	1.83	0.17	32.23	13.05	≤0.200	16.38	0.33	93.16	1.00
X38	2	—	389.50	7.65	17.22	13.70	37.17	3.05	12.30	63.43	21.56	≤0.200	≤0.300	0.24	95.84	1.50
X39	2	—	378.00	7.90	14.62	12.47	39.39	2.58	1.86	61.09	22.24	≤0.200	≤0.300	0.39	88.16	0.80
X40	2	—	369.00	7.65	15.94	13.19	34.40	2.41	11.70	59.56	21.96	≤0.200	≤0.300	0.22	88.52	1.40
X41	2	—	306.80	8.01	31.71	6.29	22.79	2.71	0.50	19.22	28.72	≤0.200	3.85	0.68	120.47	0.80
X42	2	—	355.00	7.69	33.37	13.56	10.33	5.23	0.11	31.29	62.89	≤0.200	12.18	0.18	66.70	1.00
P51	—	—	283.40	8.09	27.84	10.07	17.24	0.98	1.49	10.96	14.68	≤0.200	0.80	1.00	146.68	0.80
P114	2	—	182.80	7.63	7.35	5.20	19.41	0.81	≤0.005	9.16	26.96	≤0.200	20.56	0.09	37.62	0.60
SX1	2	—	180.90	7.70	8.45	7.01	14.58	1.04	0.07	15.33	12.37	≤0.200	25.25	0.11	39.99	0.60
SB2	3	—	249.00	8.00	25.73	6.44	16.36	0.75	12.90	8.33	26.97	≤0.200	≤0.300	0.61	110.90	0.80

^a pH measured in laboratory

Table 4 Evolution of the groundwater depth-averaged temperature depending on the total well depth

Total well depth (depth _{tot})	Mean depth-averaged temperature (°C)	SD (°C)
Depth _{tot} ≤ 10 m (17 wells)	15.4	1.9
10 m < depth _{tot} ≤ 30 m (36 wells)	17.2	1.4
Depth _{tot} > 30 m (27 wells)	17.8	1.6

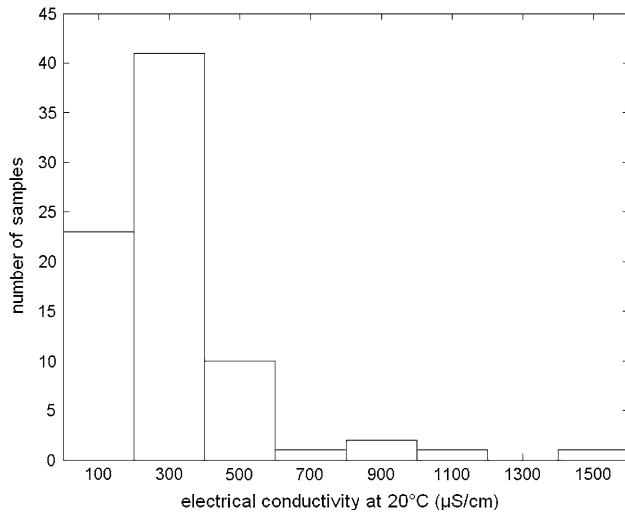


Fig. 5 Groundwater depth-averaged electrical conductivity distribution

surface required to meet the total volume of outflows. Afterwards, the risk of overdraft of groundwater resources was evaluated comparing this surface with the “Sidi Ali” spring capture zone surface.

Precipitations and evapotranspiration

The mean annual rainfall calculated from daily precipitations measured between October 1985 and September 2006 is about 635 mm. On the basis of a temperature dataset available for the same period, the potential evapotranspiration is estimated using the simple Thornthwaite formula which only requires mean monthly temperature, latitude and month (Thornthwaite and Mather 1955; Thornthwaite and Mather 1957). According to this formula which is reasonably accurate in determining mean annual values of potential evapotranspiration (Fetter 2001), the mean annual potential evapotranspiration is calculated about 879 mm.

The annual actual evapotranspiration (AEvT) is then calculated using the Thornthwaite method providing also annual available water (W_a) which is the sum of runoff (R) and infiltration (I). The main conceptual assumption of this method is that infiltration can only occur after subtracting

the needed water for evapotranspiration from a soil water storage capacity limited to a given maximum value (STO_{max}). Thus, an empirical evaluation of this STO_{max} is required. This maximum soil moisture storage capacity depends on many factors among which climate, vegetation and soil types. The values proposed in the literature (Réménieras 1986; de Marsily 1994) vary from 10 to 20 mm for a 30-cm thick sandy soil, about 100 mm for a 30-cm thick silty to clayey soil and up to 300 mm for a thin soil in arid zones. As the geology and the geomorphology of the zone are complex, a wide variety of soil types are found around the “Sidi Ali” spring. They are mainly composed of sand on the weathered granite while they are mainly composed of silt and clay on the weathered schists. Additionally, the soil thickness in the study zone can vary from 0 to 80 cm and locally up to 120 cm. Applying the Thornthwaite method, a sensitivity analysis is performed using several values for the maximum soil moisture storage capacity: 100, 175 and 250 mm. It confirms that the groundwater recharge occurs during the cold and wet period ranging from October to April. As the soil moisture storage does not reach its maximum during the driest years, it consequently appears that no groundwater recharge can be calculated during these years. The mean annual actual evapotranspiration and the mean annual available water calculated for the three values of the maximum soil moisture storage capacity are given in Table 1.

Infiltration

Considering the lack of stream hydrograph data, runoff (R) and infiltration (I) are assessed from the calculated available water (W_a). The hilly topography, the significant runoff and the observed quick response of the wadis to heavy precipitations (Fig. 4) lead to consider the runoff as systematically larger than the infiltration. Three ratios were chosen: $R = 2/3$ of W_a , $R = 3/4$ of W_a and $R = 7/8$ of W_a .

Outflows

There is no groundwater pumped by the ONEP in the capture zone of the “Sidi Ali” spring and wells. Groundwater pumped by the inhabitants of the Oulmes plateau can be considered as negligible in comparison with volumes pumped by the company for bottled mineral water and the Bâa fruit farm for irrigation. The annual volume pumped for both uses (V_{out}), estimated from a dataset of 10 years, is about 268,000 m³ among which about one-third for irrigation. Any return flow, i.e. infiltration induced by the irrigation is not considered since drip irrigation is used to avoid losses.

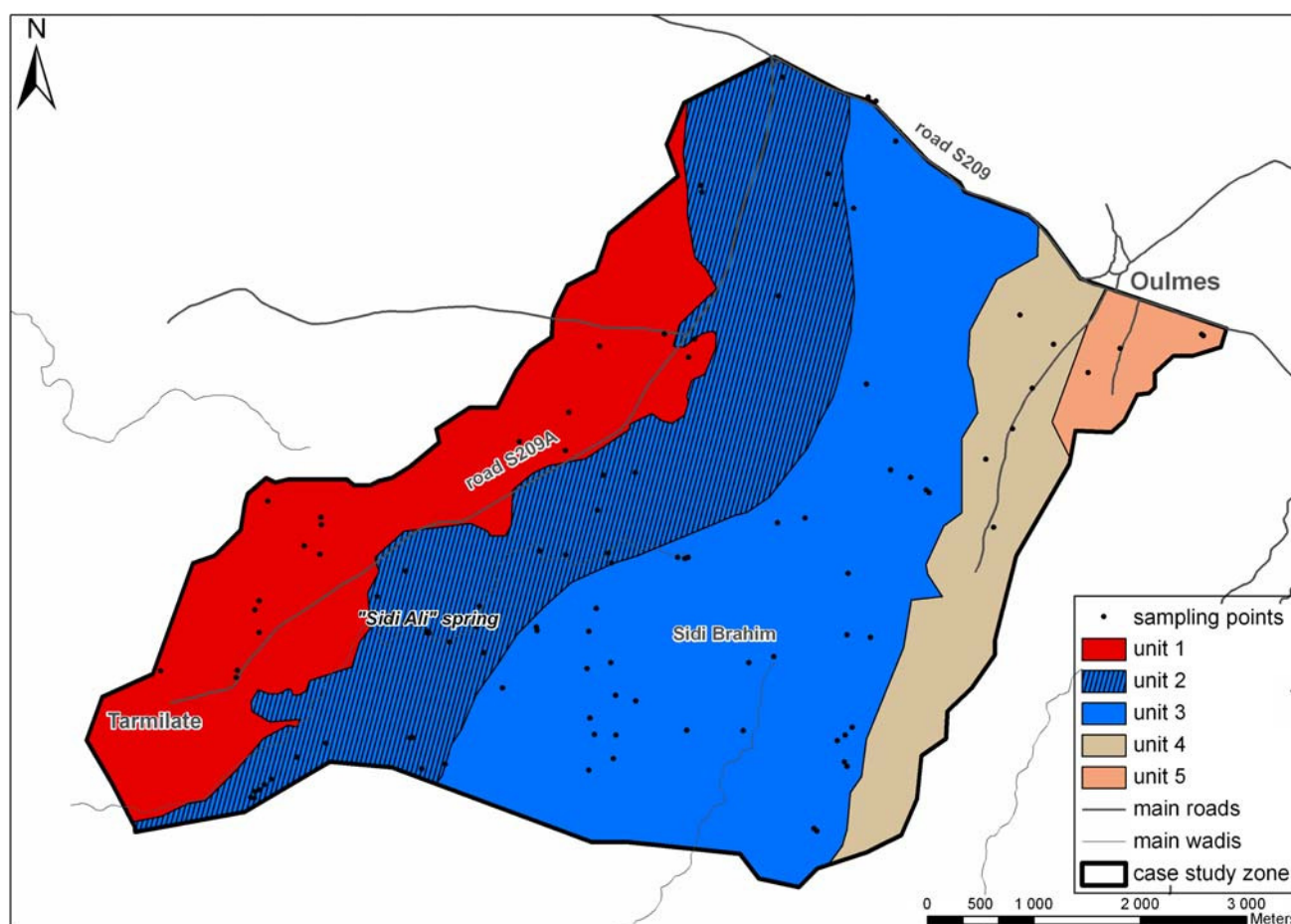


Fig. 6 Division of the study zone into five lithological units

Evaluation of possible overdraft

The term overdraft is defined as pumping in excess of the average annual recharge (Fetter 2001) which means that the sustainable extraction rate, groundwater withdrawal that satisfies water supply requirements without deleterious hydrogeological or environmental impacts (Loáiciga 2008), is exceeded. According to this definition, the risk of overdraft of the capture zone of the “Sidi Ali” spring and production wells is very simply estimated by comparing the annual infiltration with the annual pumped volumes:

$$S_{\text{required}} = \frac{V_{\text{out}}}{I}$$

where, S_{required} is the required infiltration surface to meet the total volume of outflows. This equation does not contain any baseflow term because there is almost no baseflow in the case study zone (non-perennial wadis). The mean annual runoffs, infiltrations and corresponding required infiltration surfaces are given in Table 2 for the different considered scenarios.

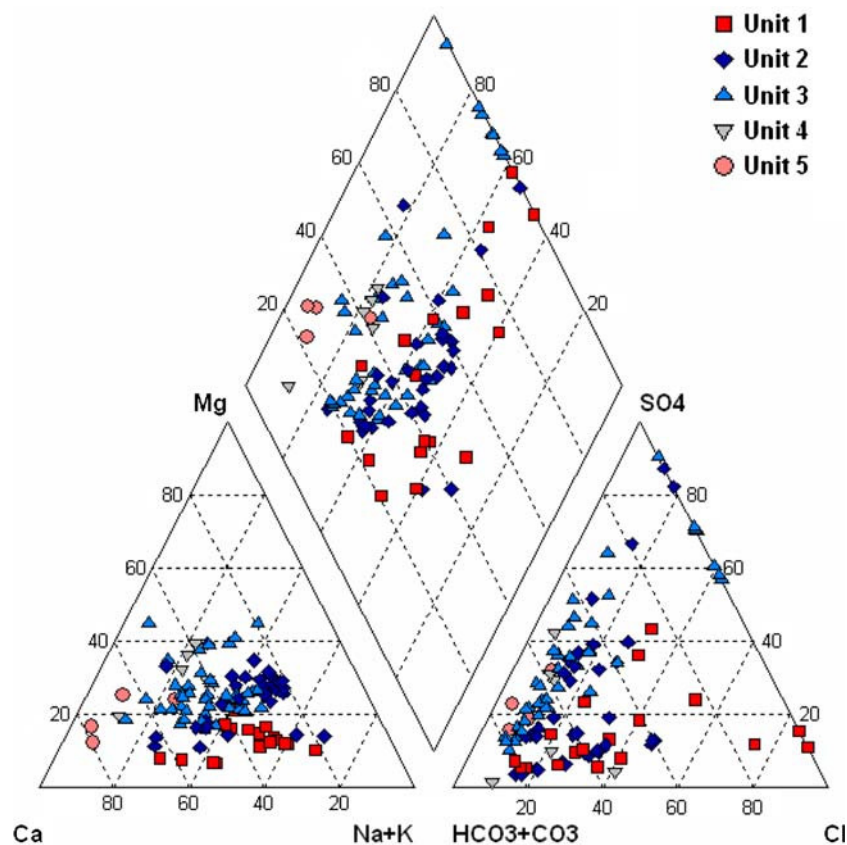
The required infiltration surfaces obtained (Table 2) compared to the capture zone of the “Sidi Ali” spring and wells evaluated from the piezometric map (10.94 km²) (Fig. 3) show that a risk of overdraft is expected in case of successive dry years when infiltration is poor or even nonexistent. According to the known volumes pumped currently, the critical infiltration under which it can be considered that groundwater pumpings are creating an overdraft is 24.45 mm/year.

Hydrogeochemistry

Temperature (T in °C), electrical conductivity at 20°C (EC in $\mu\text{S}/\text{cm}$) and concentrations in major ions (mg/l) of each groundwater sample with an acceptable error on the ion balance (maximum 5%) are given in Table 3. As almost all the samples were collected without any pumping, values are considered as representative of depth-averaged conditions.

The mean depth-averaged groundwater temperature in the study zone is 17.0°C. The corresponding SD is 1.8°C. A clear and logical dependence of the depth-averaged

Fig. 7 Piper diagram of groundwater samples classified by lithological units and showing hydrogeochemical facies



temperature on the total well depth is observed. As shown in Table 4, the highest depth-averaged temperatures correspond to the deepest wells. The mean depth-averaged groundwater electrical conductivity at 20°C in the study zone is 316 $\mu\text{S}/\text{cm}$. The corresponding SD is 225 $\mu\text{S}/\text{cm}$. This high value of SD is predominantly caused by two huge electrical conductivity values measured in two granitic arena wells and equal to 1,183 and 1,570 $\mu\text{S}/\text{cm}$. High concentrations in Na^+ (respectively, 103.2 and 288.7 mg/l), Cl^- (respectively, 156.2 and 238.9 mg/l) and NO_3^- (respectively, 279.4 and 60.9 mg/l) can explain these anomalous values. The analysis of the depth-averaged groundwater electrical conductivity distribution (Fig. 5) indicates that this parameter was lower than 200 $\mu\text{S}/\text{cm}$ for about 30% of the samples and lower than 400 $\mu\text{S}/\text{cm}$ for more than 80% of the samples. Consequently, groundwater from the capture zone of the “Sidi Ali” spring and wells is overall poorly mineralised.

Chemical species

The groundwater samples are classified into five classes according to the lithological units from where they were

sampled in the study zone (Fig. 6): unit 1—granite and granitic arena (A in Fig. 2); unit 2—highly metamorphised schists (andalusite and biotite zones) (part of B in Fig. 2); unit 3—poorly metamorphised schists (green mica and chlorite zones) (part of B in Fig. 2); unit 4—quartzites (C in Fig. 2); unit 5—shales with limestone and sandstone nodules (D in Fig. 2). Results in terms of major ions are shown in a Piper (Piper 1944) diagram (Fig. 7) for underlining possible correlation between the lithology and the observed hydrogeochemical facies.

In the cation triangle of the Piper diagram, it can be observed that 18% of the samples are of Ca-type, 70% show no dominant cation type and 12% are Na + K-type. The distribution of the samples into the different cation types depending on the lithological units is given in Table 5.

Although statistics made on units 4 and 5 could hardly be considered as completely representative (not enough samples), a correlation between cation type and lithological unit is indicated in this distribution (Table 5). Unit 1 samples show mainly waters in Na + K-type which can be related to the dissolution of feldspars such as albite and orthose contained in the granite but also waters in the Ca-type and in the no dominant cation type. The transition to units 2, 3 and 4 samples is characterised by a gradual

Table 5 Distribution of the groundwater samples into cation types depending on the lithological units

Unit	Number of samples	Samples in cation type (%)		
		Ca	Na + K	No cation dominant
1	18	22	45	33
2	33	9	12	79
3	43	16	0	84
4	6	17	0	83
5	4	100	0	0

Table 6 Distribution of the groundwater samples in anion types depending on the lithological units

Unit	Number of samples	Samples in anion type (%)			
		HCO ₃ + CO ₃	SO ₄	Cl	No anion dominant
1	18	61	0	22	17
2	33	64	9	0	27
3	43	53	26	0	21
4	6	100	0	0	0
5	4	100	0	0	0

enrichment in Ca²⁺ and Mg²⁺ against Na⁺ and K⁺ leading in majority to the no dominant cation type. Unit 5 samples are entirely included in the Ca-type waters which can be related to the dissolution of limestone nodules contained in the shales.

The anion triangle indicates that 63% are of the samples HCO₃ + CO₃-type, 13% are of the SO₄-type, 4% are Cl-type and 20% show no dominant anion type. The distribution of the samples into anion types depending on the lithological units is given in Table 6.

As for the cations and despite of few exceptions in units 4 and 5, a correlation between the dominant anion type and the lithological unit is suggested in this distribution (Table 6). Unit 1 samples show waters of the HCO₃ + CO₃-type, Cl-type and no dominant anion type. The transition to units 2 and 3 samples is characterised by a gradual enrichment of groundwater in SO₄²⁻ against Cl⁻

and, in a minor way, against HCO₃⁻ and CO₃²⁻, which can be related to the dissolution of pyrite favouring the SO₄-type. Samples of units 4 and 5 are entirely belonging to the HCO₃ + CO₃-type of water related to the dissolution of the limestone nodules contained in the shales.

Finally, the groundwater hydrogeochemical facies shown in the Piper diagram are Ca-Mg-HCO₃, Ca-Mg-SO₄-Cl, Na-K-Cl and Na-K-HCO₃ for, respectively, 57, 27, 7 and 9% of the samples. The two main facies are thus Ca-Mg-HCO₃ and Ca-Mg-SO₄-Cl since they include 84% of the samples. The distribution of the groundwater samples into the different hydrogeochemical facies depending on the lithological unit is given in Table 7.

The main facies is Ca-Mg-HCO₃ (Table 7) but a change in groundwater geochemical composition depending on the lithological units is clearly visible as the facies gradually evolves from Ca-Mg-HCO₃ to Ca-Mg-SO₄-Cl and then to Na-K-HCO₃ or Cl.

Although only few samples were available for units 4 and 5, mean concentrations in main chemical species depending on the lithological units were calculated. They are given in Table 8. A Stiff (Stiff 1951) plot showing the mean groundwater chemical composition in each lithological unit is also given (Fig. 8).

The high mean concentrations in Na⁺, Cl⁻ and NO₃⁻ in unit 1 samples underline anthropogenic effects. A severe contamination in nitrates is indeed observed in most of unit 1 samples with concentrations generally larger than 50 mg/l and locally exceeding 275 mg/l. The use of fertilizers can explain this contamination especially in the granitic arena where the sampled wells are most often shallow and located in a very permeable coarse sand grain-size formation. The concentrations in nitrates in units 2 and 3 waters are probably lower because the sampled wells in the schists are deeper and located in a lower permeable formation where reducing redox conditions induced nitrates reduction. This is confirmed by the very low concentrations (most often <1 mg/l) in nitrates measured in samples collected in the irrigation wells of the Bâa farm and in the production wells of the company "Les Eaux Minérales d'Oulmès S.A".

Table 7 Distribution of the groundwater samples in hydrogeochemical facies depending on the lithological units

Unit	Number of samples	Samples in hydrogeochemical facies (%)			
		Ca-Mg-HCO ₃	Ca-Mg-SO ₄ -Cl	Na-K-HCO ₃	Na-K-Cl
1	18	28	28	33	11
2	33	55	18	12	15
3	43	61	40	0	0
4	6	100	0	0	0
5	4	100	0	0	0

Table 8 Mean concentrations in major ions depending on the lithological units

	Unit 1	Unit 2	Unit 3	Unit 4	Unit 5
Number of samples	18	33	43	6	4
Ca ²⁺ (mg/l)	30.6	18.0	23.6	18.6	45.3
Mg ²⁺ (mg/l)	6.6	7.5	8.4	6.6	7.6
Na ⁺ (mg/l)	49.0	22.1	18.8	8.2	6.2
K ⁺ (mg/l)	4.1	3.5	2.0	1.1	1.2
Fe total (mg/l)	1.1	2.5	3.6	0.9	3.5
HCO ₃ ⁻ (mg/l)	82.5	74.9	84.9	64.3	129.2
CO ₃ ²⁻ (mg/l)	1.4	0.3	0.6	0.2	0.9
SO ₄ ²⁻ (mg/l)	28.1	28.0	43.0	16.3	30.1
Cl ⁻ (mg/l)	44.6	20.5	11.8	7.7	7.4
NO ₃ ⁻ (mg/l)	55.2	11.5	4.6	12.8	9.7

Isotopes

The content in oxygen-18 ($\delta^{18}\text{O}$ in ‰) and hydrogen-2 (δD in ‰) of samples collected over the whole Mid-Atlas and in a zone surrounding the “Sidi Ali” spring are given in Table 9.

$\delta^{18}\text{O}$

The oxygen-18 isotope allows evaluating the recharge altitude from the regional altitude isotopic gradient (Olive 1996). The regional altitude isotopic gradient of Oulmes is estimated to -0.22 ‰ per 100 m (Fig. 9) from samples collected in 15 springs and wells located over the whole Mid-Atlas region at different altitudes ranging from 300 to 2,100 m.

According to $\delta^{18}\text{O}$ concentrations, the main recharge altitude of groundwater surrounding the “Sidi Ali” spring would be about 1,200 m. Accordingly, the main recharge would occur around the principal fractured quartzitic ridge of the study zone located in the east and including several summits above 1,200 m.

$\delta^{18}\text{O}$ and δD

A comparison between the oxygen-18 isotope and the hydrogen-2 isotope allows to highlight isotopic exchanges modifying the composition of sampled groundwater in

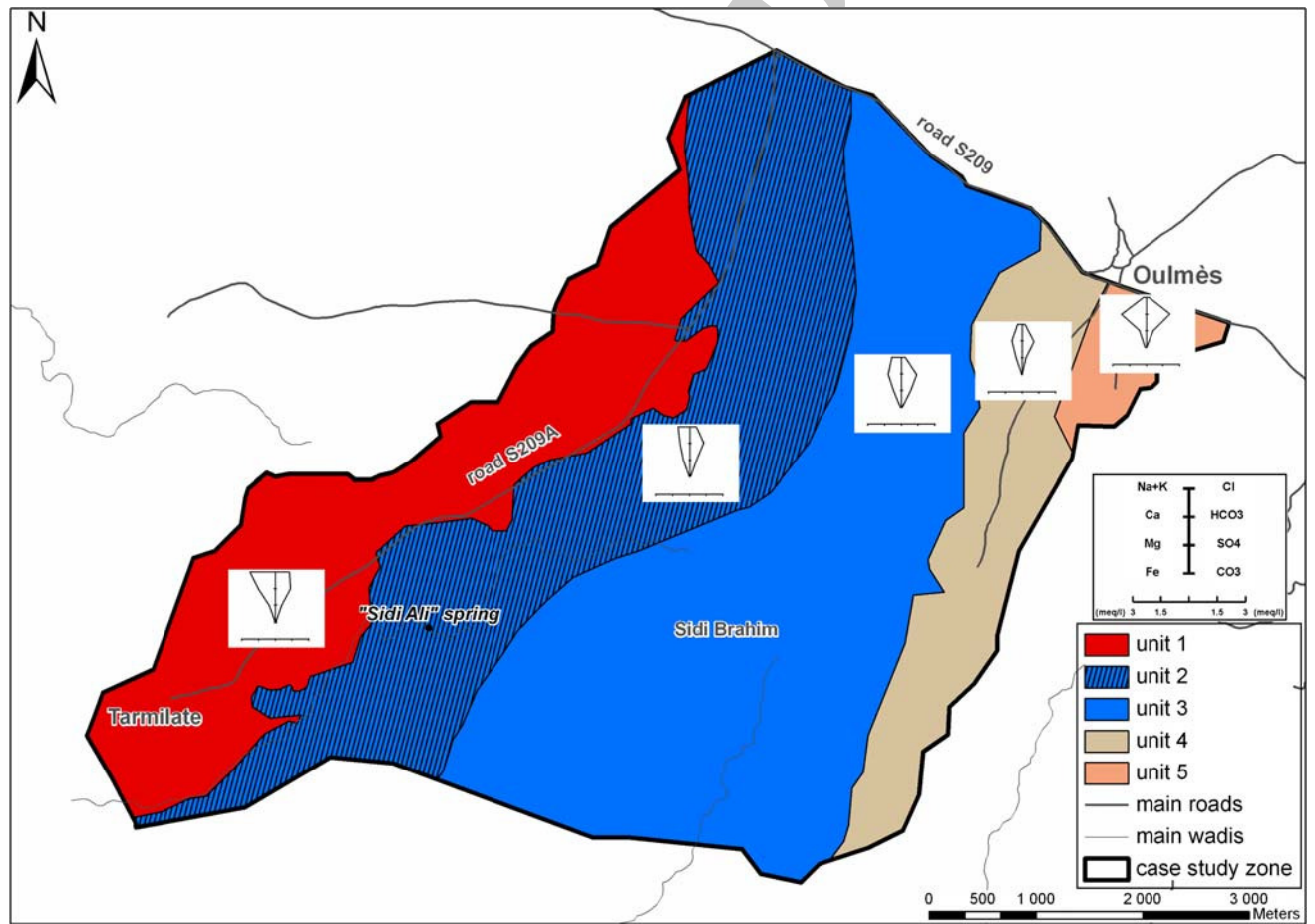
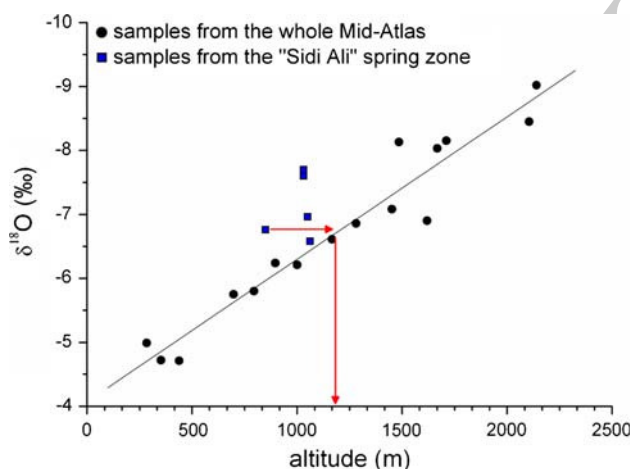


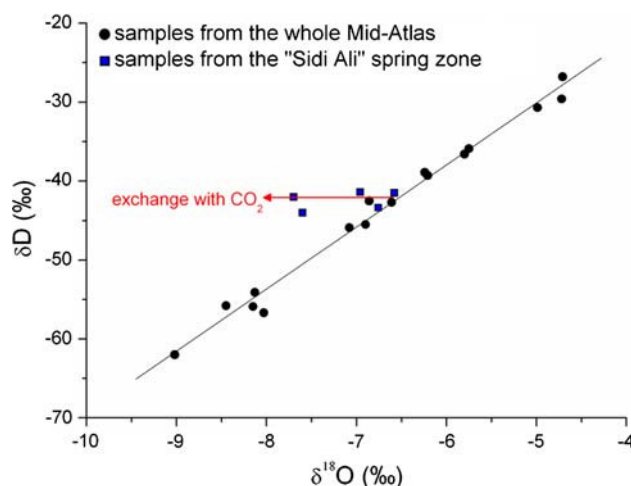
Fig. 8 Stiff plot of the mean groundwater chemical composition in each lithological unit

Table 9 Oxygen-18 ($\delta^{18}\text{O}$ in ‰) and hydrogen-2 (δD in ‰) content in samples from the whole Mid-Atlas (A–Y) and from a zone surrounding the “Sidi Ali” spring (F5 to Tam Ahamat)

ID	Altitude (m)	$\delta^{18}\text{O}$ (‰)	δD (‰)
A	897	−6.24	−38.9
AA	2,140	−9.02	−62.0
B	698	−5.75	−35.9
E	284	−4.99	−30.7
G	795	−5.80	−36.6
H	1,166	−6.61	−42.7
I	1,000	−6.21	−39.3
J	1,485	−8.13	−54.1
L	1,711	−8.15	−55.9
O	1,668	−8.03	−56.7
Q	1,619	−6.90	−45.5
U	439	−4.71	−26.8
V	352	−4.72	−29.6
W	1,281	−6.86	−42.5
X	1,451	−7.08	−45.9
Y	1,205	−8.45	−55.8
F5	1,030	−7.60	−44.0
Pz5	1,030	−7.70	−42.0
SA	1,062	−6.58	−41.5
Ain Karrouba	1,050	−6.96	−41.4
Tam Ahamat	850	−6.76	−43.4

**Fig. 9** Altitude isotopic gradient of the Oulmes plateau

oxygen-18 isotope (Olive 1996; Akouvi et al. 2008). The local meteoric water line (LMWL) (Fig. 10) of the region is estimated to be: $\delta\text{D} = 8 \delta^{18}\text{O} + 9$ ‰. Very similar to the World Meteoric Water Line (WMWL) defined by Craig (1957), this linear relation with a gradient of eight indicates that the chemical composition of sampled groundwater was not significantly modified by evaporation.

**Fig. 10** Local Meteoric Water Line (LMWL)

Graphically, the position of the samples surrounding the “Sidi Ali” on the left of the LMWL suggests an isotopic exchange which modifies their isotopic composition. This one can only occur between CO_2 and H_2O via the equilibrium $\text{C}^{16}\text{O}_2 + \text{H}_2^{18}\text{O} \leftrightarrow \text{C}^{16}\text{O}^{18}\text{O} + \text{H}_2^{16}\text{O}$. The corresponding equilibrium fractionation factor at 100°C is:

$$\varepsilon^{18}\text{O}_{\text{CO}_2-\text{H}_2\text{O}} = \frac{[\text{O}^{18}/\text{O}^{16}]_{\text{CO}_2}}{[\text{O}^{18}/\text{O}^{16}]_{\text{H}_2\text{O}}} = 1,030$$

This fractioning indicates CO_2 enriching in ^{18}O against H_2O . This enrichment, estimated to 1‰ for the Oulmes plateau groundwater, requires high concentrations in CO_2 suggesting a magmatic origin. The possibility of CO_2 rising up from the granite through the fissured schists was confirmed by a borehole drilled in the highly metamorphised schists (andalusite zone) where CO_2 gas was measured at a concentration of 2 g/l.

^{13}C and ^{14}C

The carbon-13 and carbon-14 isotopes allow separating total dissolved carbon (C_{tot}) into carbon from biological origin (C_{bio}) and carbon from mineral (magmatic) origin (C_{min}) (Olive 1996). Standard values of C_{bio} and C_{min} in terms of ^{13}C and ^{14}C concentrations are given in Table 10.

The ^{13}C content measured in the carbonates of highly metamorphised schists is −9.6 ‰. The ^{13}C and ^{14}C concentrations in samples collected in wells of the company “Les Eaux Minérales d’Oulmès S.A” surrounding the “Sidi Ali” spring are given in Table 11.

Considering these values and the corresponding graph (Fig. 11), C_{min} would constitute about 30–50% of C_{tot} in

Table 10 ^{13}C and ^{14}C contents (standard values) in biological carbon (C_{bio}) and mineral carbon (C_{min})

	^{13}C (‰)	^{14}C (pCm)
C_{bio}	-22	100
C_{min}	-3.5 ^a	0
Carbonates of the highly metamorphised schists	-9.6	-

^a ^{13}C concentration measured on gas in Lalla Haya by Winckel (2002)

Table 11 Measured ^{13}C and ^{14}C concentrations in wells surrounding the “Sidi Ali” spring

Well ID	^{13}C (‰)	^{14}C (pCm)
F5	-11.7	48.9 ± 0.8
F6	-16.5	77.6 ± 1
Pz5	-11.9	45.1 ± 0.6

groundwater surrounding the “Sidi Ali” spring which confirms once more that gas is rising up from the granite through the schists.

Another process likely to produce CO_2 is decarbonation at high temperature. This possibility is negligible in this case study since there is almost no carbonate in the highly metamorphised schists (Table 10). Additionally, if a decarbonation process producing a CO_2 enriched of 1–2 ‰ in ^{13}C , was active, the ^{13}C concentration measured in Lalla Haya should be about -8 ‰ instead of the measured -3.5 ‰ (Table 10). Consequently, such a process can be considered as inactive in the study zone.

^{14}C and ^3H

Carbon-14 isotope and hydrogen-3 isotope allow estimating the mean age of groundwater (Olive 1996; 2000). Although there is magmatic CO_2 gas rising up, groundwater from the study zone should be relatively young since ^{14}C concentrations measured in samples collected in wells of the company “Les Eaux Minérales d’Oulmès S.A” (Table 11) indicate that groundwater surrounding the “Sidi Ali” spring is younger than 200 years. On the other hand, the ^3H concentrations measured in the same wells (Table 12) suggest that groundwater surrounding the “Sidi Ali” spring is older than 50 years since only younger groundwater (or mixing of old and young groundwater) would contain more than 2 TU (Fig. 12). According to ^{14}C and ^3H concentrations, groundwater from the case study zone should be aged from about 50 to 200 years.

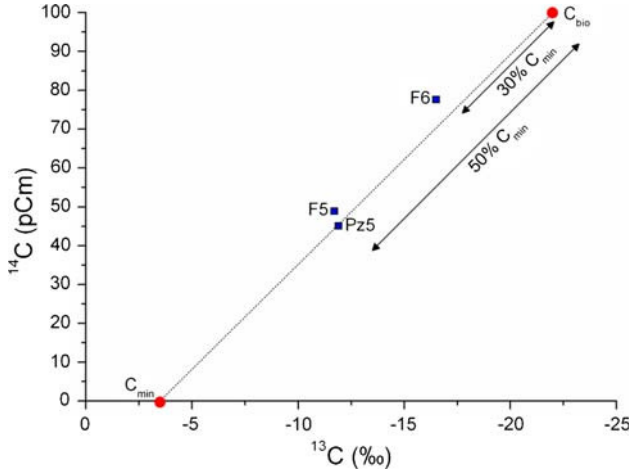


Fig. 11 ^{13}C and ^{14}C concentrations in C_{bio} , C_{min} and wells surrounding the “Sidi Ali” spring

Table 12 ^3H concentration in wells surrounding the “Sidi Ali” spring

Well ID	T (TU)
F5	≤ 1.9
Pz5	≤ 2.4

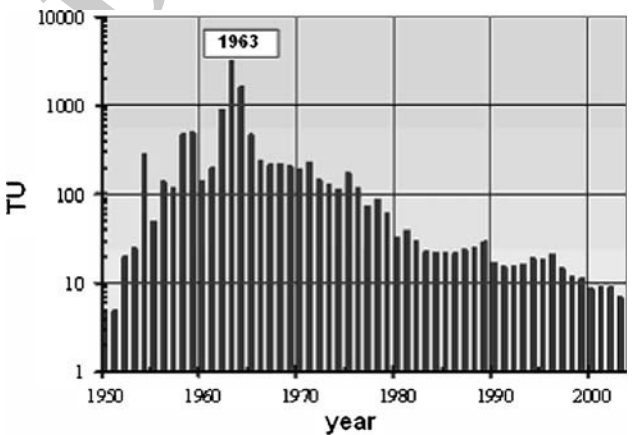


Fig. 12 ^3H concentration measured in precipitations in Thonon-les-Bains since 1950

Discussion

About piezometry (Fig. 3), this study confirms the general trends observed on the partial piezometric maps obtained in the less extensive previous studies: the piezometric depression in the centre of the study zone and the groundwater flow direction westwards along the eastern slope of the principal ridge. According to this piezometric map, water recharge can mainly occur in the upward zone at an altitude of the plateau between about 1,175 and 1,250 m. The saturated zone is reached at an altitude between approximately 1,150 and 1,200 m. A confirmation

is provided by the isotope analyses indicating that a mean recharge altitude of about 1,200 m (Fig. 8) corresponding to the upward part of the catchment and to the main ridge of the Oulmes plateau constituted by fractured quartzites.

A specific discussion point must be addressed about the possible partitioning of the considered aquifer in low piezometric conditions. Static piezometric heads measured in some wells close to each others are quite different during the irrigation period (a difference of 3 m at a distance of 30 m) while they are nearly similar (i.e. in equilibrium) in winter. This observation confirms that in dry and irrigation conditions, the hydrogeological system can be considered as functioning with two separated aquifers: a deep and large extension aquifer and shallow and small capacity perched aquifer compartments. Conversely, after winter recharge, respective piezometric heads in the regional deep aquifer and in the shallow compartments cannot be distinguished.

Clear correlations between hydrogeochemical facies and lithology are demonstrated despite a high heterogeneity in groundwater chemical composition in each lithological unit. Although the Ca–Mg–HCO₃ groundwater facies remains predominant, it progressively evolves along the main flow path of the study zone since the Ca–Mg–HCO₃, Ca–Mg–SO₄–Cl and Na–K–HCO₃ or Cl facies appear, respectively, in the fractured quartzites, the poorly metamorphosed schists and the highly metamorphosed schists and the granite and granitic arena (Table 7).

As interpreted from the isotope analyses, groundwater from the capture zone of the “Sidi Ali” spring and wells results from a mixing of “young” water coming from the recharge with “old” water with dissolved gas rising up from the granite through the schists. A schema summarising the hydrogeological functioning of the “Sidi Ali” spring according to the results obtained in this study is proposed in Fig. 13.

Conclusion

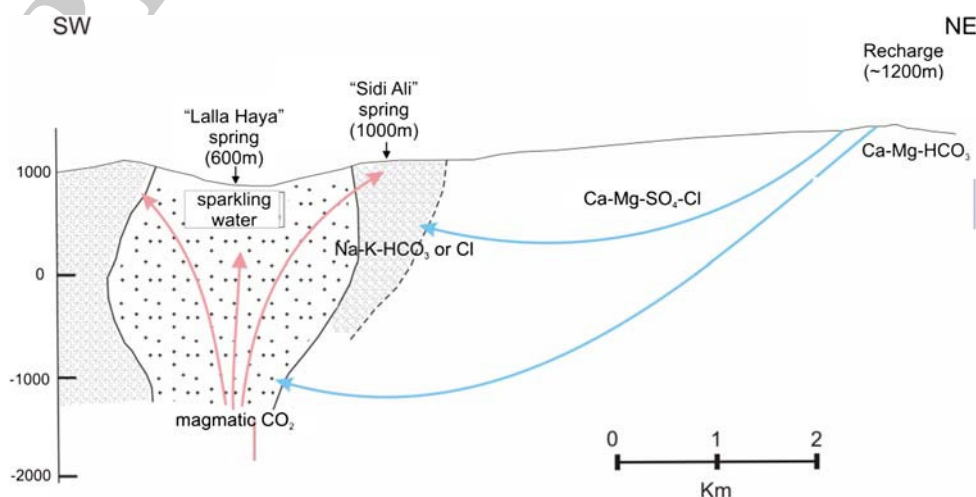
A new hydrogeological study, performed from a large set of recent data mainly collected in a zone surrounding the “Sidi Ali” spring, allows to improve the conceptual understanding of the complex Oulmes fractured hydrogeological system. This system, located in schists metamorphosed by a surrounding granite, appeared to be constituted by a main deep aquifer of large extension and by minor aquifers with a small capacity in a perched position with regards to the main deep aquifer. Clearly separated during the dry and irrigation period, the deep and the shallow aquifers interact enough to be in total equilibrium after the winter recharge. The origin of groundwater is mainly infiltration water except, as highlighted by isotopes, a small part of old groundwater with dissolved gas rising up from the granite through the schists.

Piezometric and isotopic data show that the recharge occurs mainly at an altitude of about 1,200 m corresponding to the principal ridge of the study zone made of fractured quartzites. Furthermore, a main flow path starts from this ridge to go westwards to the centre of the plateau. Although the main hydrogeochemical facies observed in the Piper diagram is Ca–Mg–HCO₃, an evolution of the groundwater facies is visible along this main flow path since Ca–Mg–SO₄–Cl and Na–K–HCO₃ or Cl facies appear when the schists and the granite and granitic arena are reached.

An intense exploitation of groundwater resources, especially for mineral water bottling and irrigation, could lead to overdraft only in case of successive dry years when the winter recharge is poor or nonexistent.

Concerning the quality of groundwater, a severe contamination in nitrates is observed in wells drilled in the granite and the granitic arena. This contamination is not observed in the schists, probably because nitrates are

Fig. 13 Schema of the hydrogeological functioning of the “Sidi Ali” spring



reduced in this anoxic media. However, this last statement can be biased by the fact that most of the wells drilled in the schists are deeper and more protected than those drilled in the granite and the granitic arena.

Acknowledgments Authors are grateful to the company “Les Eaux Minérales d’Oulmès S.A” for supporting this study and the needed field campaigns.

References

- Agard J, Termier H, Odowenko B (1950) Les gîtes d’étain et de tungstène de la région d’Oulmès (Maroc Central), vol 82. Editions du Service Géologique du Maroc, Rabat 326
- Akouvi A, Dray M, Violette S, de Marsily G, Zuppi GM (2008) The sedimentary coastal basin of Togo: example of a multi-layered aquifer still influenced by a palaeo-seawater intrusion. *Hydrogeol J* 16(3):419–436
- Baudin T, Roger J, Chèvremont P, Rachdi H, Chenakeb M, Cailleux Y, Razin P, Bouhdadi S (2001) Carte géologique du Maroc (1/50 000)—Feuille d’Oulmès. Editions du Service Géologique du Maroc, Rabat
- Beaudet G (1969) Le Plateau Central Marocain et ses bordures: études géomorphologiques. Ph.D. Thesis, Université de Paris, Paris, p 478
- Boutaleb M (1988) Reconstitution de l’évolution tectono-métamorphique, magmatique et hydrothermale du district stannowolframifère de Walmès (Maroc Central)—implications métallogéniques. Ph.D. Thesis, Nancy, Institut National Polytechnique de Lorraine, p 310
- Craig H (1957) Isotopic standards for carbon and oxygen and correlation factors for mass spectrometric analysis of carbon dioxide. *Geochim Cosmochim Acta* 12:133–149
- Dadi S (1998) Contribution à l’étude hydrologique et hydrochimique du Plateau d’Oulmès (Maroc Central, Maroc). Ph.D. Thesis, Université Cadi Ayyad, Marrakech, p 182
- de Marsily G (1994) Hydrogéologie: comprendre et estimer les écoulements souterrains et le transport de polluants. Pierre et Marie Curie, Université Paris VI, Paris

- Diot H, Bouchez J-L, Boutaleb M, Macaudière J (1987) Le granite d’Oulmès (Maroc Central): structures de l’état magmatique à l’état solide et modèle de mise en place. *Bulletin de la Société Géologique de France* numéro spécial 3(1):157–168 (série 8)
- Fetter CWJ (2001) Applied hydrogeology. Pearson education. Prentice-Hall, Upper Saddle River, p 598
- Gmira A (1996) Altération des granites d’Oulmès (Maroc Central), vol 139. Documents du Laboratoire Géologique de Lyon, Lyon, p 148
- Lagarde J-L (1985) Cisaillements ductiles et plutons granitiques contemporains de la déformation hercynienne post-viséenne de la Méséta Centrale. *Hercynia* 1–1:29–37
- Loáiciga HA (2008) Aquifer storage capacity and maximum annual yield from long-term aquifer fluxes. *Hydrogeol J* 16:399–403
- Michard A (1976) Eléments de géologie marocaine, vol 252. Editions du Service Géologique du Maroc, Rabat, p 408
- Olive P (1996) Introduction à la géochimie des eaux continentales. Editura Didactică I Pedagogică, Bucurest, p 127
- Olive P (2000) La datation des eaux souterraines à long temps de résidence par le radiocarbonate Mode d’emploi. *Hydrogéologie* 1:3–19
- Piper AM (1944) A graphic procedure in the geochemical interpretation of water analyses. *Trans Am Geophys Union* 25:914–923
- Réménieras G (1986) L’hydrologie de l’ingénieur, 2nd edn. Eyrolles, Paris
- Stiff HAJ (1951) The interpretation of chemical water analysis by means of patterns. *J Petrol Technol* 3:15–17
- Tahiri A (1991) Le Maroc Central Septentrional: stratigraphie, sédimentologie et tectonique du Paléozoïque; un exemple de passage des zones internes aux zones externes de la chaîne hercynienne du Maroc. Ph.D. Thesis, Université de Bretagne Occidentale, Brest, p 300
- Termier H (1936) Etudes géologiques sur le Maroc central et le Moyen Atlas septentrional, vol 33. Editions du Service Géologique du Maroc, Rabat, p 1566
- Thorntwaite CW, Mather JR (1955) The water balance. *N.J. Lab Climatol Publ* 8:1–86
- Thorntwaite CW, Mather JR (1957) Instructions and tables for computing potential evapotranspiration and the water balance. *N.J. Lab Climatol Publ* 10:185–311